

CrystEngComm

Accepted Manuscript



This is an *Accepted Manuscript*, which has been through the Royal Society of Chemistry peer review process and has been accepted for publication.

Accepted Manuscripts are published online shortly after acceptance, before technical editing, formatting and proof reading. Using this free service, authors can make their results available to the community, in citable form, before we publish the edited article. We will replace this *Accepted Manuscript* with the edited and formatted *Advance Article* as soon as it is available.

You can find more information about *Accepted Manuscripts* in the [Information for Authors](#).

Please note that technical editing may introduce minor changes to the text and/or graphics, which may alter content. The journal's standard [Terms & Conditions](#) and the [Ethical guidelines](#) still apply. In no event shall the Royal Society of Chemistry be held responsible for any errors or omissions in this *Accepted Manuscript* or any consequences arising from the use of any information it contains.

Gallic acid–Succinimide Co-crystal landscape: Polymorphism,
Pseudopolymorphism, Variable Stoichiometry Co-crystals and Concomitant
Growth of Non-solvated and Solvated Co-crystals†

Ramanpreet Kaur, Suryanarayan Cherukuvada, Praveen B. Managutti and Tayur N. Guru
Row*

Solid State and Structural Chemistry Unit, Indian Institute of Science,
Bengaluru 560012, India

*Email: ssctng@sscu.iisc.ernet.in

Abstract

The structural landscape of the binary gallic acid–succinimide combination has been explored. A recently reported dimorphic 1:2 co-crystal is shown by differential scanning calorimetry (DSC) to exhibit a third polymorph at high temperature. Further, seven solvated co-crystals have been obtained, including three different hydrates (gallic acid:succinimide:water in 1:1:1, 2:2:1 & 2:4:1 ratios) and solvates with 1,4-dioxane (1:1:1), tetrahydrofuran (2:2:1), acetone (2:2:1) and ethyl acetate (3:3:1) respectively. A rare phenomenon of concomitant solvation besides concomitant polymorphism in the 1:2 co-crystal is recognized, which posed difficulties in obtaining phase-pure crystal forms in bulk quantity. Based on structural insights, methods to obtain pure co-crystals and design of several solvates are suggested. Additionally, a 1:1 co-crystal, which had been elusive under ambient conditions, is found to show polymorphic behavior for the materials obtained under nitrogen atmosphere and by high temperature desolvation of several solvates as analyzed by powder X-ray diffraction (PXRD) and DSC.

Introduction

The study of structural landscape has major implications in comprehending the crystal form diversity of molecular solids and is therefore of importance in terms of both fundamental and application facets.¹ It facilitates the understanding of the crystallization process and can assist in the design of a desired solid form. The landscape of an organic system encompasses polymorphs, its multi-component adducts such as solvates, co-crystals, and even its homologues and analogues.^{1b-1} In the context of co-crystals being more amenable to design and having immense potential for tailored solutions in areas like pharmaceuticals,² organic

synthesis and separation,³ optoelectronics⁴ etc., studies on landscape of these systems are deemed important. Gallic acid (abbreviated as GA, Figure 1) is a dietary polyphenolic acid and possesses anti-oxidant, anti-microbial and anti-cancer properties, apart from its usage for various applications in drug industry.⁵ The potential to form varied and multiple hydrogen bonding motifs with its carboxylic acid and three hydroxyl groups allow for polymorphism, pseudopolymorphism, solvatomorphism and co-crystal polymorphism of gallic acid.^{4c,6} Braun et al.^{6b} studied the crystal energy landscape of gallic acid and its monohydrate and successfully obtained polymorphs of gallic acid which were elusive for over seventy years since their discovery. Driven by this background and our own studies^{4c,6d-f} on the diversity and applications of gallic acid crystal forms, further studies on gallic acid co-crystals have been undertaken to investigate the factors responsible for rich structural diversity exhibited by this system. Herein, we report polymorphism, pseudopolymorphism and variable stoichiometry co-crystals of gallic acid–succinimide (GA–SM) combination.

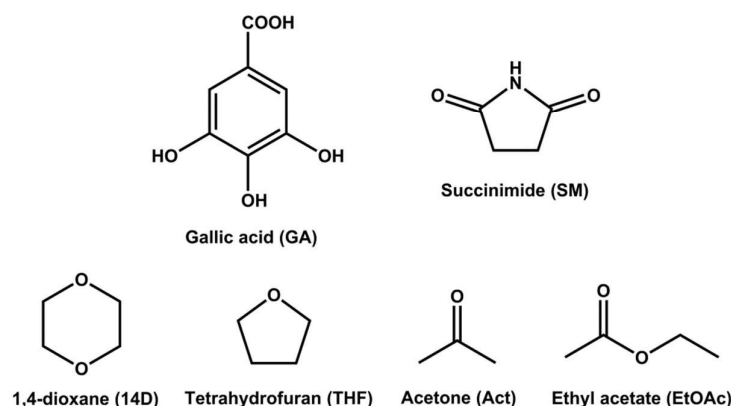


Figure 1 Molecular structures and acronyms of the components of gallic acid–succinimide adducts.

In a co-crystallization experiment, the combination of internal (presence of various/multiple hydrogen bonding groups, mismatch of donor-acceptor ratio, awkward shape and conformational freedom of molecule) and external factors (crystallization conditions such as solvent, temperature, supersaturation, solution kinetics) gives rise to multifarious possibilities of supramolecular association such that the outcome of co-crystallization becomes less predictable; the product can altogether be a new polymorph/pseudopolymorph/solvate/co-crystal/co-crystal solvate or a concomitant mixture of any of these.^{1,6d,f,7} Hence, the formation of polymorphs, hydrates/solvates, variable stoichiometry co-crystals, multiple *Z'* structures, salt co-crystals, solvates of co-crystals/salts

can be considered a nemesis^{7e,f} to crystal engineering because of the unpredictability associated and lesser design control. Although each of these materials have their own importance, what is paramount from a practical outlook is to zero-in to a particular material in the landscape and gain control over its formation. In the present study, gallic acid with its three hydroxyl groups can invoke various supramolecular motifs to give rise to various kinds of adducts since the influence of hydroxyl group is three fold: (i) its strength and structure directing effect, (ii) its bent nature presenting both donor and acceptor sites for hydrogen bonding and (iii) its conformational flexibility.^{4c,6b-f,8} Herein, a rare phenomenon of concomitant manifestation of solvates,⁹ including hydrates, along with the polymorphs of 1:2 GA–SM (represented as 2:1 SM–345THBA in our previous study^{6f}) co-crystal is observed. Polymorphic and hydrate impurities are of major concern for pharmaceuticals, from production to consumption, because of physical property and intellectual property issues involved.^{7f,g,m,10} This warrants the development of a methodology to generate the desired solid form devoid of impurity. In this study, we describe the efforts undertaken to obtain the materials in a phase-pure state. Furthermore, polymorphic behavior of 1:1 GA–SM co-crystal obtained under non-ambient conditions is also discussed.

Results and Discussion

Co-crystallization experiments of GA–SM combination were performed by mechanochemical grinding (both neat and liquid-assisted grinding)¹¹ and evaporative crystallization^{2e,7f} methods (detailed in the Experimental Section) and Table 1 enlists the polymorphs and solvates of the combination. It is noteworthy that a concomitant mixture of polymorph I of 1:2 co-crystal and a solvated co-crystal (Table 1) was always obtained and attempts to obtain 1:1 GA–SM co-crystal were unsuccessful. It appears that the conditions tried were not right for the crystallization of 1:1 cocrystal. On the other hand, polymorph II of 1:2 co-crystal, despite being more stable than polymorph I from energy calculations (Table 2), did not crystallize in significant amounts. Neat/liquid-assisted (NG/LAG) grinding of 1:1 GA–SM at ambient conditions resulted in the formation of 1:1:1 hydrate as confirmed by PXRD (Figure 2) and TGA (Figure 3). NG/LAG of GA–SM 1:2 stoichiometry exclusively resulted in metastable polymorph I of 1:2 co-crystal (Figure 4). In all, phase-pure 1:1 co-crystal and stable polymorph II of 1:2 co-crystal could not be obtained from routine crystallization experiments. In principle, it should be possible to obtain 1:1 co-crystal by desolvation as the majority of solvated co-crystals have GA and SM in equal stoichiometries (Table 1). Indeed, we were successful in obtaining the same upon careful desolvation of several solvates (1:1:1 GA–SM–

water, 1:1:1 GA–SM–dioxane and 3:3:1 GA–SM–ethyl acetate) at elevated temperatures (Table 1), apart from neat grinding of the combination in nitrogen atmosphere. The structural reasons for the concomitant solvation of GA–SM co-crystal are discussed first, followed by X-ray crystal structures of solvates and then the characterization of 1:1 GA–SM co-crystal and polymorph III of 1:2 GA–SM co-crystal in the subsequent sections.

Table 1 Co-crystallization results of GA–SM combination.

Stoichiometry	Method		Result
1:1	Solution crystallization	methanol	1:2 GA–SM co-crystal polymorph I + 1:1:1, 2:2:1 and 2:4:1 GA–SM hydrates
		1,4-dioxane	1:2 GA–SM co-crystal polymorph I + 1:1:1 GA–SM–14D solvate
		THF	1:2 GA–SM co-crystal polymorph I + 2:2:1 GA–SM–THF solvate
		acetone	1:2 GA–SM co-crystal polymorph I + 2:2:1 GA–SM–Act solvate
		ethyl acetate	1:2 GA–SM co-crystal polymorph I + 3:3:1 GA–SM–EtOAc solvate
		DMF and DMSO	1:2 GA–SM co-crystal polymorphs I and II
	Neat grinding		1:1:1 GA–SM hydrate
Water-assisted grinding		1:1:1 GA–SM hydrate	
1:2	Neat grinding		1:2 GA–SM co-crystal polymorph I
	Independent water-, DMF- and DMSO-assisted grinding		1:2 GA–SM co-crystal polymorph I
Solvate	Desolvation temperature		Result
1:1:1 GA–SM–water	75 °C		1:1 GA–SM co-crystal
1:1:1 GA–SM–dioxane	140 °C		
3:3:1 GA–SM–ethyl acetate	70 °C		

Table 2 Lattice energy calculations of 1:2 GA–SM polymorphs.^a

E value	Polymorph I	Polymorph II
E(bulk) (Hartrees)	–5468.5286	–2734.5617
E(mol) (Hartrees)	–1366.9715	–1367.1141
E(mol, ghost) (Hartrees)	–1366.9841	–1367.1281
ΔE(cond) (Hartrees)	–0.1607	–0.1666
BSSE (Hartrees)	0.0126	0.0139
E(cohesive energy) (Hartrees)	–0.1480	–0.1527
E(cohesive energy) (Kcal/mol)	–92.9207	–95.8607

^a(see Experimental Section)

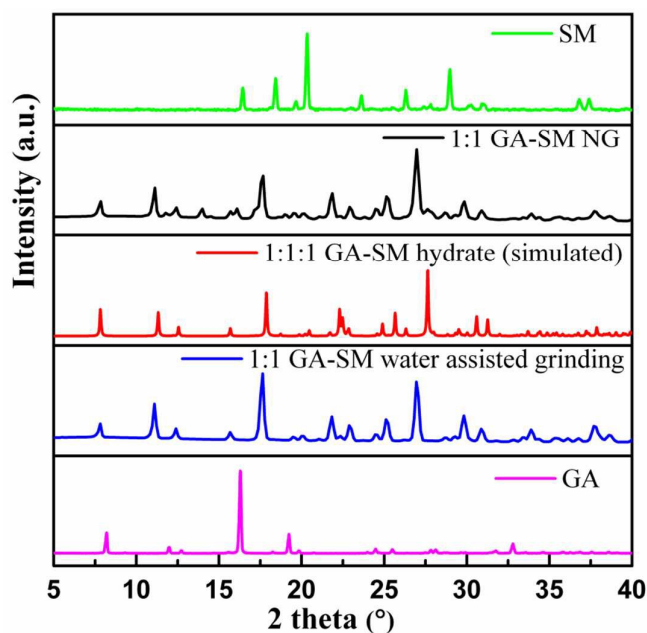


Figure 2 PXRD of 1:1 GA–SM neat ground (NG) material (black) is distinct from that of parent materials, GA (magenta) & SM (green), and shows good match with the simulated X-ray diffraction pattern of 1:1:1 GA–SM hydrate (red). 1:1 GA–SM water ground material (blue) shows complete match with the same. Peaks of simulated (110 K) and experimental (298 K) patterns at higher angles are offset to each other due to temperature difference.

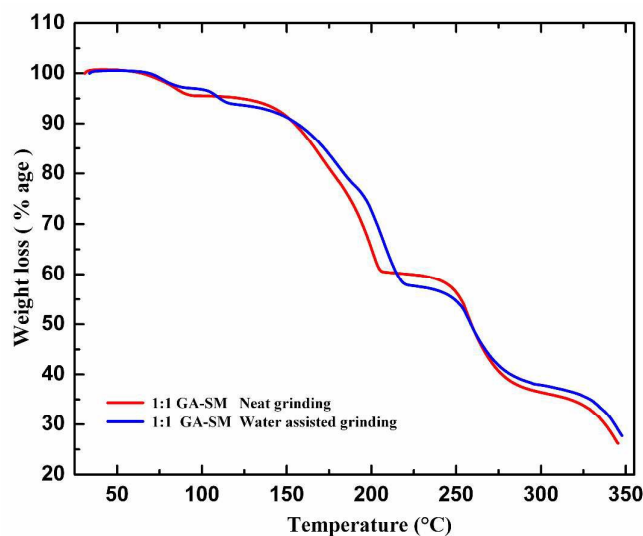


Figure 3 TGA of 1:1 GA–SM neat ground (red) and water ground (blue) materials. The weight proportion of one water molecule in 1:1:1 GA–SM hydrate is 6.2% and the former shows weight loss of 5% indicating partial water absorption and partial formation of hydrate. The latter with 6% weight loss shows complete hydrate formation.

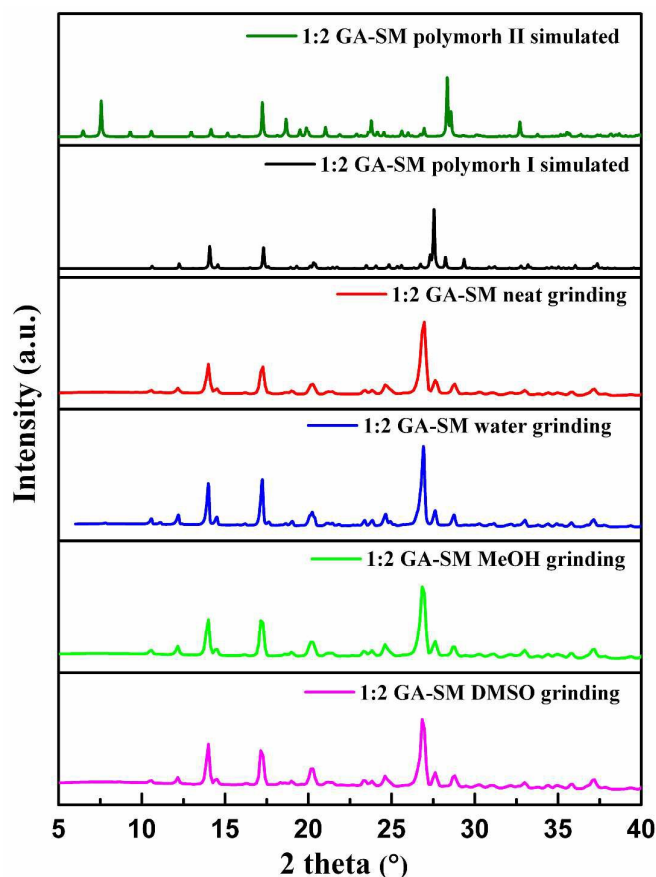
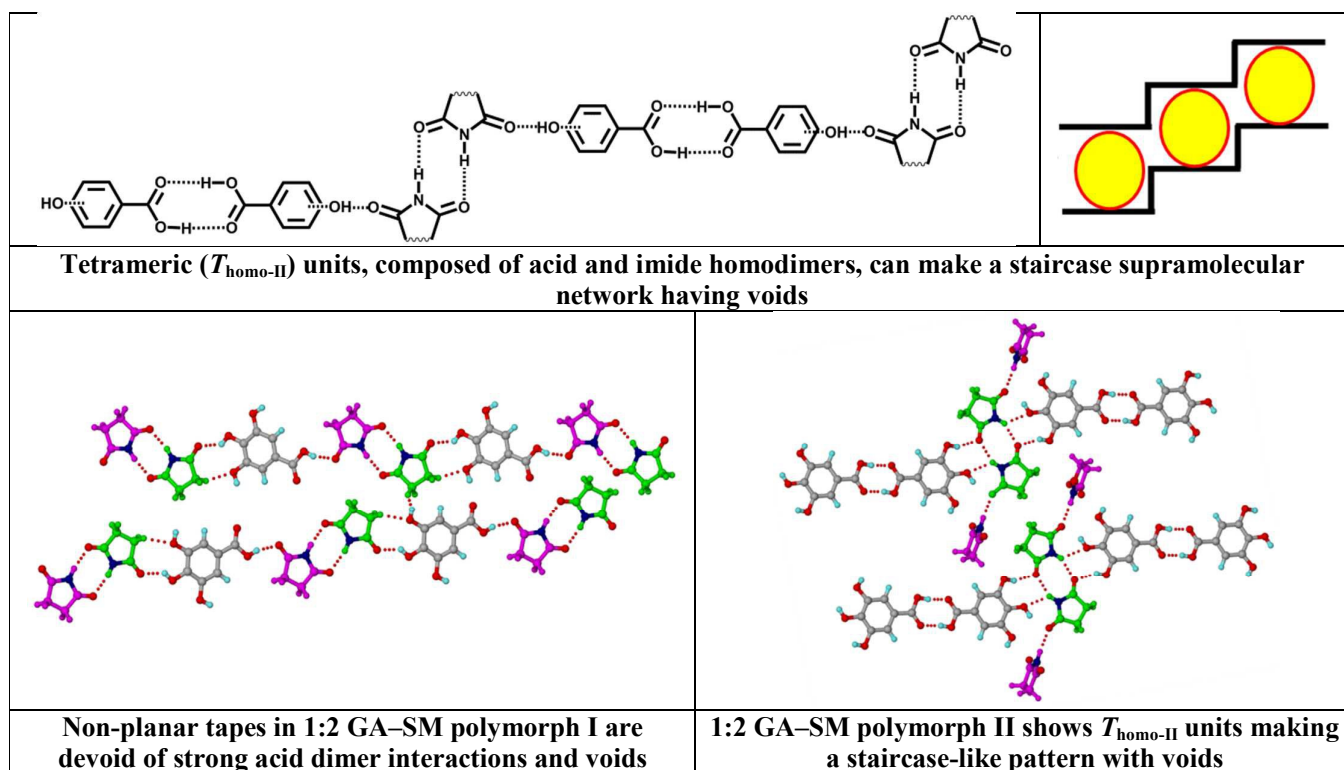


Figure 4 PXR D of 1:2 GA–SM neat ground and water/methanol/DMSO ground materials respectively exhibit complete match with the simulated X-ray diffraction pattern of 1:2 GA–SM co-crystal polymorph I.

A. GA–SM co-crystal solvates and non-formation of 1:1 co-crystal and polymorph II of 1:2 co-crystal:

The supramolecular basis for the formation of all solvates can be understood based on the design schematics for 1:1 acid–imide co-crystals in our recent study.^{6f} Among various supramolecular motifs, the tetrameric unit, named as $T_{\text{homo-II}}$ unit,^{6f} composed of carboxylic acid_(GA) and carboximide_(SM) homodimers (Figure 5), connected by hydroxyl_(GA)⋯imide_(SM) interactions appears to be energetically favorable. These $T_{\text{homo-II}}$ units can generate a staircase supramolecular assembly containing voids (Figure 5) to allow for the accommodation of solvent molecules. Indeed, crystal structure analysis of the obtained GA–SM solvated co-crystals shows that all are manifested with the same void-containing staircase network (Figure 5) manifesting a void volume of $\sim 40 \text{ \AA}^3$. This leads to the inference that the tendency of 1:1 combination to form void-containing supramolecular assembly as the cause for the

non-formation of non-solvated 1:1 GA–SM co-crystal. On the other hand, although polymorph II of 1:2 GA–SM co-crystal features $T_{\text{homo-II}}$ units akin to solvated co-crystals (Figure 5), it did not crystallize in significant amounts. In this context, the occurrence of a rare phenomenon of concomitant crystallization of 1:2 GA–SM co-crystal polymorph I and a solvated co-crystal (Table 1) is of particular interest. This can be explained based on 'Ostwald's rule of stages'.¹² The crystallization broth is a heterogeneous medium where many kinds of supramolecular assemblies are possible; in the competition between different motifs to crystallize out, kinetic forms get preferred more often. Among the solvated motifs and non-solvated motifs, the former crystallizes first and exhibits a dominant growth though both motifs comprise of similar units; among the non-solvated motifs, the one with feeble interactions emerges in majority. Thus, the solvated co-crystal and less stable 1:2 GA–SM polymorph I crystallize concomitantly as compared to polymorph II, irrespective of the solvent and 1:1 stoichiometry of the components used. Crystallographic parameters of the solvates and hydrates are given in Table 3.



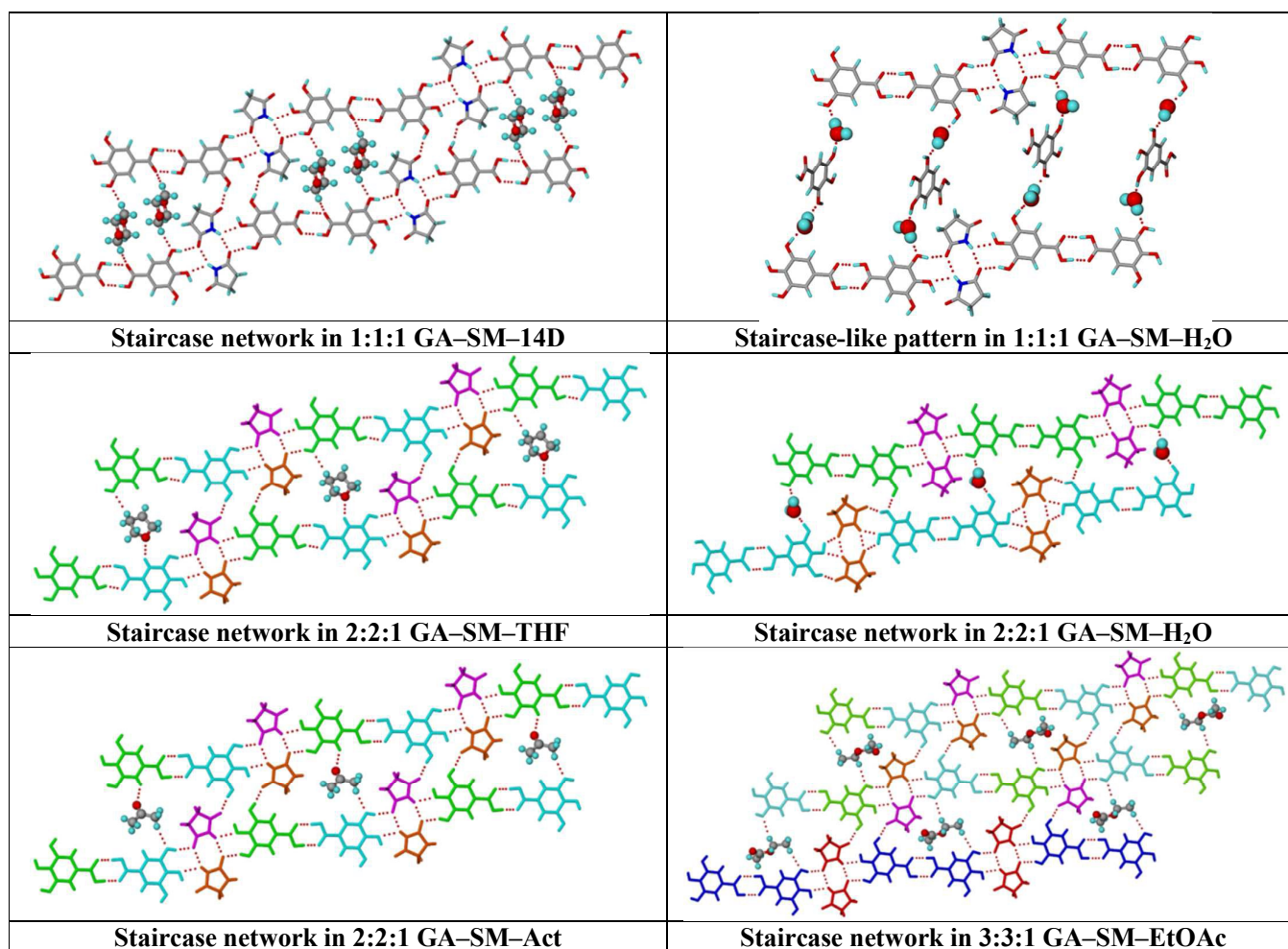


Figure 5 Tetrameric $T_{\text{homo-II}}$ unit, composed of carboxylic acid and carboximide homodimers, serves as a building block for staircase network containing voids in 1:1 carboxylic acid-carboximide combinations. Water molecules are held in voids through O-H \cdots O interactions and other solvents through C-H \cdots O interactions in their respective solvates. Symmetry independent molecules are shown in different color.

Table 3 Crystallographic parameters of all solvates and hydrates of GA–SM system.^a

Adduct	1:1:1 GA–SM–14D	2:2:1 GA–SM–THF	2:2:1 GA–SM–Act	3:3:1 GA–SM–EtOAc	1:1:1 GA–SM–H ₂ O	2:2:1 GA–SM–H ₂ O	2:4:1 GA–SM–H ₂ O
Formula	C ₁₃ H ₁₅ NO ₈	C ₂₆ H ₃₀ N ₂ O ₁₅	C ₂₅ H ₂₈ N ₂ O ₁₅	C ₃₇ H ₃₉ N ₃ O ₂₃	C ₁₁ H ₁₃ N ₁ O ₈	C ₂₂ H ₂₄ N ₂ O ₁₅	C ₃₀ H ₃₄ N ₄ O ₁₉
Formula weight	313.26	610.52	596.49	893.71	287.22	556.43	754.61
CCDC number	1413790	1413796	1413794	1413795	1413791	1413792	1413793
Temperature (K)	120(2)	110(1)	110(1)	110(2)	110(2)	120(1)	110(2)
R(int)	0.0268	0.0284	0.0310	0.0405	0.0372	0.0680	0.0663
Crystal system	Triclinic	Triclinic	Triclinic	Triclinic	Monoclinic	Triclinic	Triclinic
Space group	<i>P</i> $\bar{1}$	<i>P</i> 1	<i>P</i> $\bar{1}$	<i>P</i> $\bar{1}$	<i>P</i> 2 ₁ / <i>c</i>	<i>P</i> $\bar{1}$	<i>P</i> $\bar{1}$
<i>a</i> (Å)	4.948(1)	5.927(5)	8.276(1)	9.132(1)	4.735(1)	8.070(1)	11.490(1)
<i>b</i> (Å)	10.576(1)	8.342(5)	11.689(1)	14.045(1)	16.341(1)	10.345(1)	13.167(1)
<i>c</i> (Å)	13.891(1)	13.899(5)	14.765(1)	15.506(1)	15.621(1)	15.391(1)	13.308(1)
α (°)	109.5(1)	79.8(1)	108.3(1)	79.4(1)	90	103.0(1)	67.52(1)
β (°)	95.5(1)	84.0(1)	97.7(1)	85.3(1)	91.5(1)	91.1(1)	67.49(1)
γ (°)	101.8(1)	77.4(1)	101.7(1)	79.2(1)	90	109.4(1)	64.74(1)
Volume (Å ³)	660.0(1)	658.6(7)	1297.7(1)	1917.8(1)	1208.3(1)	1174.4(1)	1623.5(2)
<i>Z</i>	6	10	10	14	12	10	14
Density (g cm ⁻³)	1.58	1.54	1.526	1.55	1.58	1.57	1.54
μ (mm ⁻¹)	0.133	0.128	0.128	0.131	0.137	0.135	0.131
F (000)	328	320	624	932	600	580	788
<i>h</i> _{min,max}	-6, 6	-8, 8	-10, 10	-11, 11	-5, 5	-9, 9	-14, 14
<i>k</i> _{min,max}	-13, 12	-12, 11	-14, 14	-18, 18	-16, 20	-12, 12	-16, 16
<i>l</i> _{min,max}	-17, 17	-20, 21	-18, 18	-20, 20	-13, 19	-18, 18	-16, 16
No. of measured reflections	8239	16853	16178	27372	4986	20774	28566
No. of unique reflections	2581	8553	5101	8795	2366	4609	6385
No. of reflections used	2282	7113	4253	5136	1692	3488	5069
No. of parameters	219	421	421	629	209	400	534
<i>R</i> _{all} , <i>R</i> _{obs}	0.039, 0.034	0.056, 0.044	0.049, 0.040	0.105, 0.059	0.073, 0.046	0.074, 0.056	0.058, 0.044
<i>wR</i> _{2_all} , <i>wR</i> _{2_obs}	0.086, 0.083	0.117, 0.107	0.111, 0.104	0.187, 0.154	0.101, 0.087	0.157, 0.141	0.120, 0.108
$\Delta\rho_{\text{min,max}}$ (e Å ⁻³)	-0.201, 0.298	-0.293, 0.445	-0.273, 0.225	-0.483, 0.532	-0.258, 0.229	-0.413, 0.310	-0.322, 0.266
GOOF	1.035	1.035	1.037	1.019	1.012	1.060	1.053

^a *Z* = *Z*' (no. of crystallographically non-equivalent molecules of any type in the asymmetric unit)¹³ × no. of independent general positions of the space group

B. Pseudopolymorphs of GA–SM co-crystal

Three different stoichiometry hydrates (1:1:1, 2:2:1 and 2:4:1) of GA–SM co-crystal were obtained concomitantly with polymorph I of 1:2 co-crystal upon crystallization of 1:1 GA–SM from methanol (see Table 1). Remarkably, all the three hydrates possess the same staircase supramolecular network with voids occupied by water molecules (Figures 5 & 6).

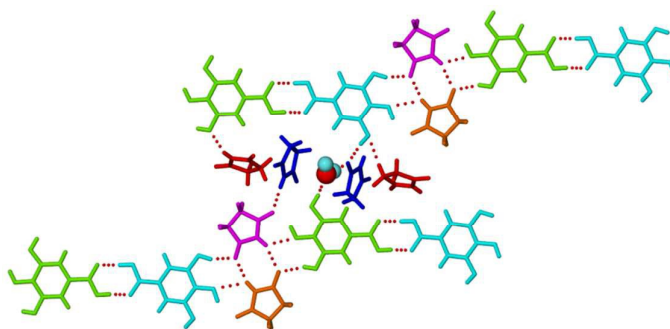


Figure 6 Staircase network in 2:4:1 GA–SM–water. Symmetry independent molecules are shown in different color.

Among other GA–SM co-crystal solvates, at first, 1,4-dioxane and acetone solvates were obtained. Based on the structural similarity between 1,4-dioxane and tetrahydrofuran on one hand and acetone and ethyl acetate on the other, respective solvates were anticipated and indeed obtained. They have different stoichiometries (GA–SM–THF in 2:2:1 and GA–SM–EtOAc in 3:3:1 ratios) as compared to GA–SM–14D (1:1:1) and GA–SM–Act (2:2:1) solvates respectively (Tables 1 & 3; Figure 5). Interestingly, all these solvates always crystallize concomitantly with polymorph I of 1:2 GA–SM co-crystal and also exhibit the same supramolecular network. 2:2:1 GA–SM–THF and 1:1:1 GA–SM–14D are nearly isomorphous with interchange of unit cell axes and angles (see Table 3). 2:2:1 GA–SM–Act shows a doubling of *a*-axis and corresponding doubling of unit cell volume with respect to 1:1:1 GA–SM–14D. 3:3:1 GA–SM–EtOAc shows doubling of *a*-axis and 1.5 fold increase in *b*-axis resulting in a corresponding tripling of the unit cell volume with respect to 1:1:1 GA–SM–14D. Further, 3:3:1 GA–SM–EtOAc shows almost 1.5 fold increase of *b*-axis and corresponding 1.5 fold increase of unit cell volume with respect to 2:2:1 GA–SM–Act (Table 3). It is noteworthy that the structures of 2:2:1 and 3:3:1 solvated co-crystals show that the excess GA–SM stoichiometries which correspond to unique molecules have no effect on the overall crystal packing as compared to 1:1:1 dioxane co-crystal (Figure 5). Independent liquid-assisted grinding experiments of 1:1 GA–SM using 1,4-dioxane, ethyl acetate,

tetrahydrofuran and acetone reproduced the respective solvated co-crystals as established by PXRD (Figure 7). GA–SM–THF and GA–SM–Act solvates have formed only when dry solvents were used and especially under nitrogen atmosphere, otherwise 1:1:1 GA–SM hydrate was always obtained. It is to be noted that such conditions are not the case with dioxane and ethyl acetate solvates which could be easily obtained. The affinity of THF and acetone, apart from 1:1 GA–SM combination, for water should be the reason for the formation of hydrate in ambient conditions for those cases.

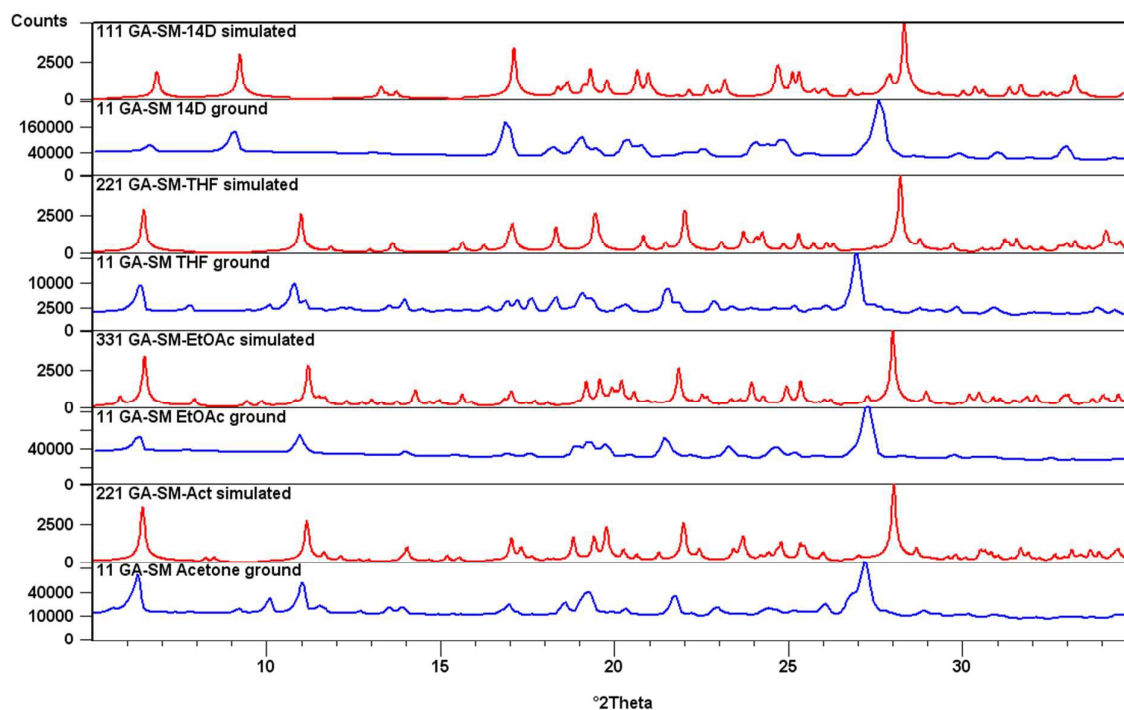


Figure 7 PXRD of GA–SM solvate materials obtained upon grinding (blue traces) from respective solvents show good match with the simulated X-ray diffraction patterns (red traces) of corresponding solvated co-crystals. Peaks of simulated (110 K) and experimental (298 K) patterns at higher angles are offset to each other due to temperature difference.

To see whether the supramolecular motifs found in common in the solvates are modular and translate into their ability for solvent exchange, we have performed solvent exchange experiments on 1:1:1 GA–SM hydrate, 1:1:1 GA–SM–14D and 3:3:1 GA–SM–EtOAc independently. Since isolating single crystals of solvates has been cumbersome because of concomitant crystallization, bulk powders were used for experiments. Each of the solvate powder materials were subjected to independent vapor diffusion (detailed in the

Experimental Section) and LAG experiments with other solvents (1:1:1 GA–SM hydrate independently with 1,4-dioxane and ethyl acetate; 1:1:1 GA–SM–14D with water and ethyl acetate; 3:3:1 GA–SM–EtOAc with water and 1,4-dioxane) and analyzed by PXRD. The transformation of a given solvate to other solvate was found to be facile and reversible. This confirms the robustness of $T_{\text{homo-II}}$ units in GA–SM combination to generate void-containing supramolecular assemblies for solvent incorporation as well as exchange. The final observation from these experiments is that GA–SM combination displays extensive hydration tendency along with an ability to form several solvates.

C. Characterization of 1:1 GA–SM co-crystal

The preferential formation of supramolecular motifs based on $T_{\text{homo-II}}$ units as seen above seem to hinder the formation of 1:1 GA–SM co-crystal at ambient conditions (even in solvent less conditions of neat grinding; see Figure 2). The fact that nitrogen atmosphere facilitated the formation of THF and acetone solvated co-crystals, which are otherwise inaccessible due to hydration tendency of GA–SM combination, led us to attempt neat grinding of the combination under nitrogen atmosphere to access the elusive 1:1 co-crystal. Our efforts have successfully resulted in the formation of a 1:1 co-crystal as evaluated by PXRD (Figure 8), DSC & TGA (Figure 9) analyses of the ground material. On the other hand, the higher stoichiometry solvated co-crystals viz. 2:2:1 GA–SM–THF/Act/H₂O and 3:3:1 GA–SM–EtOAc, which are in principle solvates of 1:1 co-crystal, besides the 1:1:1 GA–SM–H₂O/14D, can be induced to lose solvent and consequently generate a solvent-free 1:1 GA–SM co-crystal. DSC and TGA experiments were performed on 1:1:1 GA–SM–H₂O/14D and 3:3:1 GA–SM–EtOAc solvates to know the possibility of generating pure 1:1 GA–SM co-crystal at elevated temperatures. TGA of these solvates showed two-step weight loss events (one before 130 °C and other between 150-200 °C, Figure 10) and DSC corroborated the events by showing two endothermic phase transitions followed by a common melting endotherm around 200 °C (Figure 10). The first weight loss corresponds to loss of respective solvent apparently leaving behind GA–SM in 1:1 stoichiometry between 130-150 °C after which there was weight loss to result in a non 1:1 stoichiometry. Controlled desolvation of the solvates was carried out in an oven at 130 °C for an hour and the resultant materials were analyzed by PXRD. Powder diffractograms of all the three heated materials were different from the starting materials (both solvates and pure components) and also the 1:1 cocrystal obtained under nitrogen atmosphere (Figure 8) but exhibited complete match with each other (Figure 11) illustrating that the desolvated solvates manifest as a distinct phase. NMR purity

check of desolvated materials established their integrity as a 1:1 co-crystal. To further validate the formation of 1:1 co-crystal, we ground the material with an extra mole of SM and obtained the 1:2 co-crystal polymorph I (Figure 12) and water-assisted grinding of the material resulted in 1:1:1 GA–SM–water. Altogether, it is of interest to note that even the 1:1 co-crystal, which had been elusive under ambient conditions, shows polymorphic behavior as per the PXRD and thermal analyses of the materials obtained under nitrogen atmosphere and by desolvation.

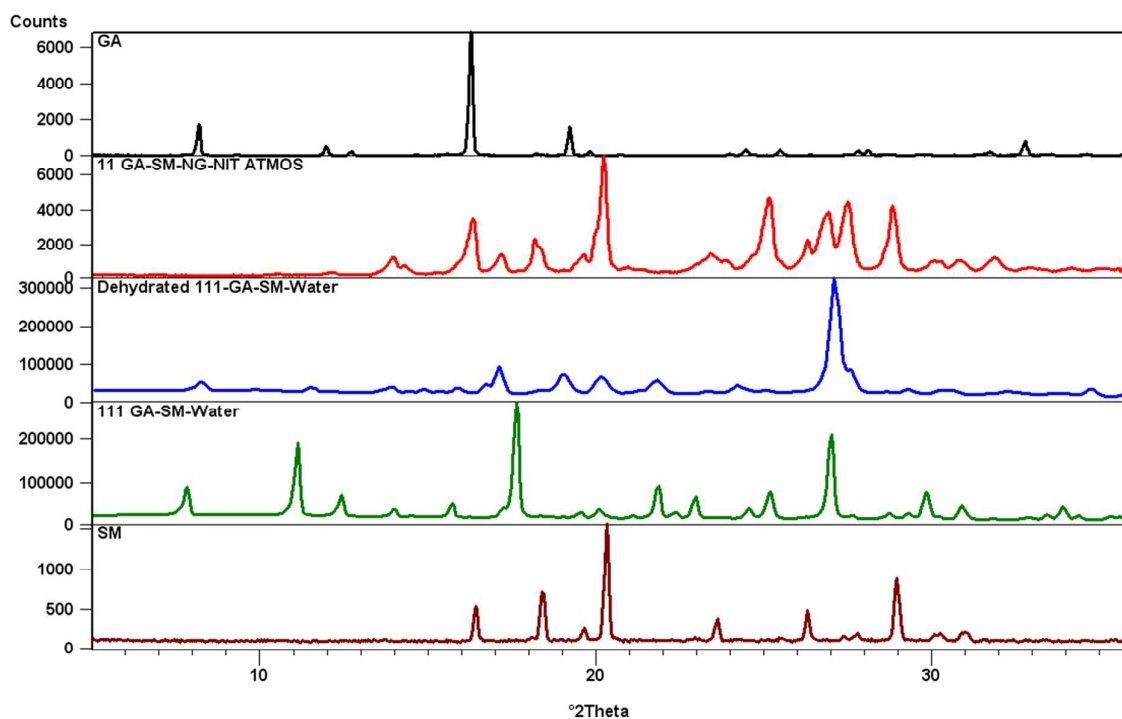


Figure 8 PXRD of 1:1 GA–SM ground material under nitrogen atmosphere (red) and of dehydrated 1:1:1 GA–SM–water (blue) are different from each other and are also distinct from that of GA (black), SM (brown) and 1:1:1 GA–SM hydrate (green).

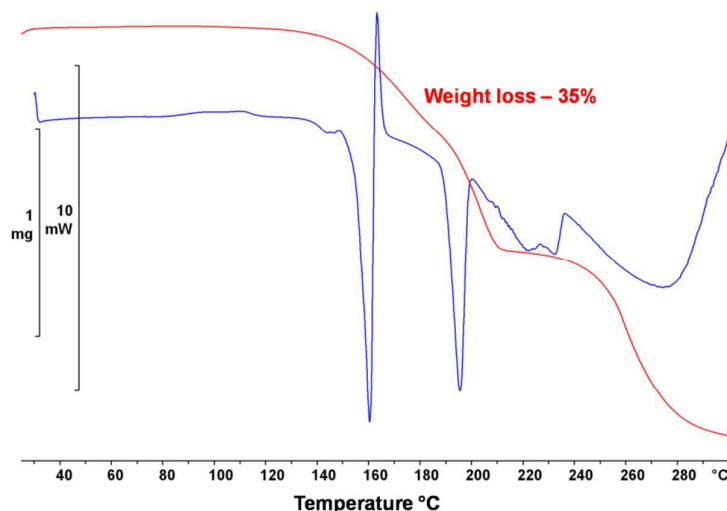


Figure 9 DSC (blue) and TGA (red) of 1:1 GA–SM co-crystal obtained under nitrogen atmosphere. The material shows two major endotherms (160 & 195 °C) with an exotherm (165 °C) in between in the DSC. The weight loss of 35% up till 195 °C appears to correspond to two events viz. (i) dissociation and release of SM from 1:1 co-crystal and (ii) decomposition of GA component plausibly to pyrogallol (1,2,3-trihydroxybenzene formed by release of carbon dioxide from GA; new peaks in NMR spectra matched with reported pyrogallol peaks).^{8a} Both these events are partial and the stoichiometry of 1:1 GA–SM became 1:0.66 at melting.

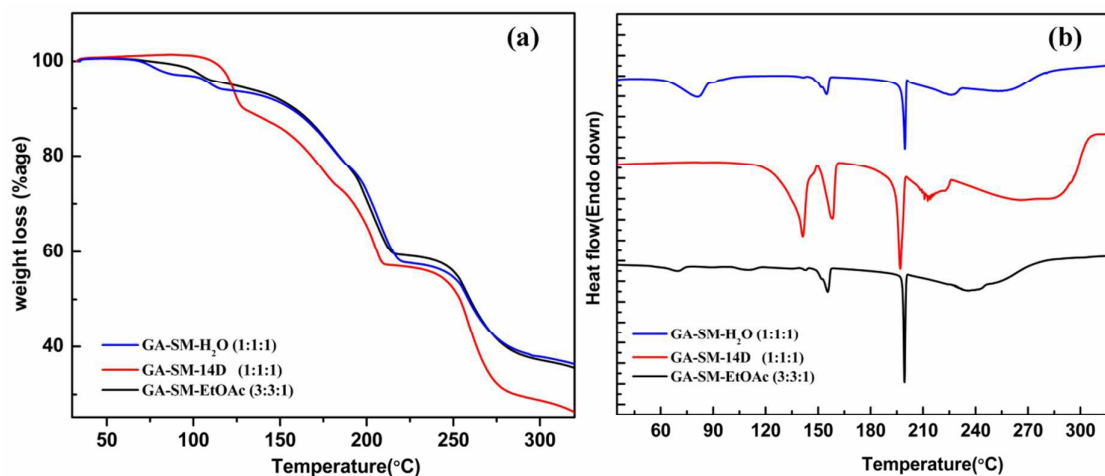


Figure 10 TGA (a) and DSC (b) analysis of GA–SM solvates. Thermal transitions up till 130 °C correspond to loss of respective solvent (calculated vs. observed weight loss: 1:1:1 GA–SM–H₂O - 6.22% vs. 6.2%; 1:1:1 GA–SM–14D - 24.6% vs. 20.3%; 3:3:1 GA–SM–EtOAc -

9.8% vs. 10.2%) to give a desolvated 1:1 GA–SM phase. Past desolvation, the weight loss of about 35% corresponds to two events as mentioned in Figure 9.

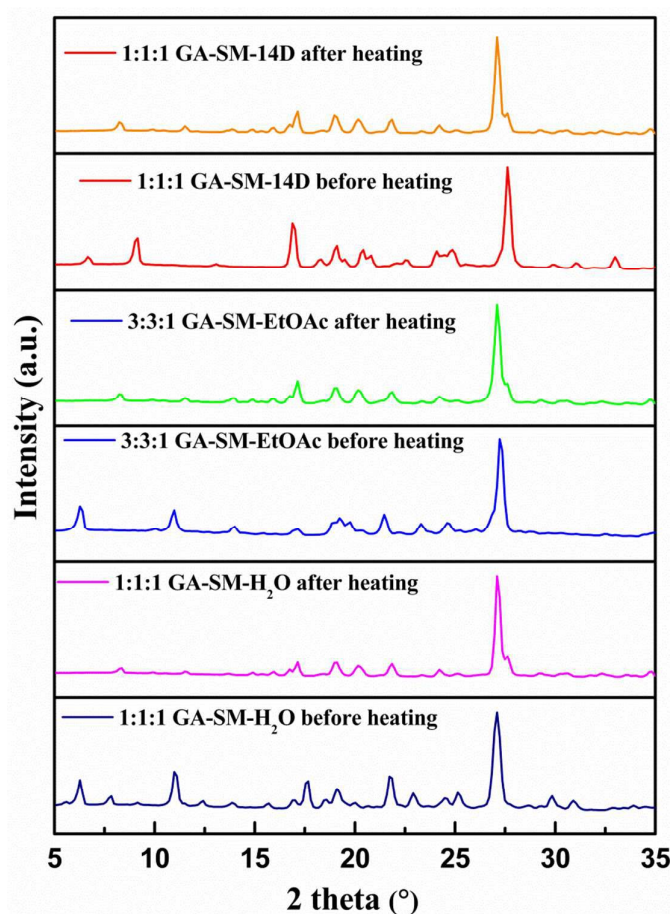


Figure 11 PXR D patterns of GA–SM solvates before heating and after heating at $130\text{ }^{\circ}\text{C}$. All the solvates after heating show complete match with each other indicating the formation of the same 1:1 desolvated solvate material in common.

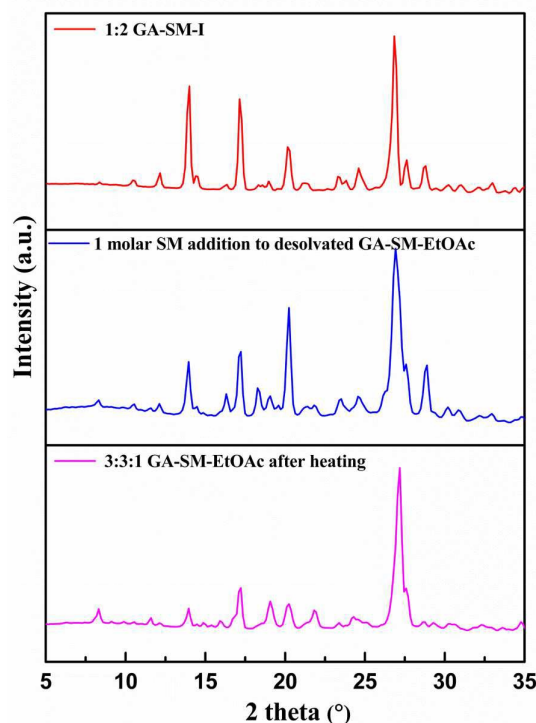


Figure 12 PXR D of desolvated 3:3:1 GA–SM–EtOAc solvate (magenta). PXR D of ground mixture of desolvated solvate + 1 mol SM (blue) matches with 1:2 GA–SM co-crystal polymorph I (red).

D. Third polymorph of 1:2 GA–SM co-crystal

Interestingly, attempts to establish the stability relationship between the dimorphs of the co-crystal led to the discovery of a third polymorph. Polymorph I was harvested as the major product from various crystallization experiments and polymorph II was obtained in small quantities from DMF and DMSO mediated crystallization (Table 1). This observation, apart from lattice energy calculations (see Table 2), supports the kinetic nature of polymorph I as well as the stable nature of polymorph II based on the generality that high boiling point solvents tend to facilitate the formation of stable polymorphs.¹⁴ Carboxylic acid dimers and multiple O–H···O interactions involving imide carbonyl acceptors in polymorph II as compared to single-point interactions in polymorph I seem to lower the energy for the former, which is ~3 Kcal/mol more stable than the latter (Table 2). DSC, which is known to deduce the thermal stability order among polymorphs,¹⁵ was carried out on both polymorphs. Polymorph I showed an endothermic transition around 144 °C just before melting (158 °C), whereas polymorph II showed clean melting (Figure 13a). However, TGA of polymorph I showed no weight loss (Figure 13a) thus indicating a possible polymorphic transformation

and no solvent loss or sublimation. When the polymorph was subjected to high heating rate, which minimizes polymorphic transformations, it's pure melting event was observed (black trace in Figure 13a). It was found to have ~ 8 kJ/mol (or 2 Kcal/mol) lower heat of fusion compared to polymorph II ($\Delta H_{\text{fus}} = 47.4$ vs. 55.5 kJ/mol; Table 4), thus establishing polymorph II as the stable form. Heat-cool cycle DSC experiment on polymorph I showed a reversible phase transition with an exothermic peak (cooling run) in the same temperature regime as that of endothermic peak (heating run, Figure 13b). This suggests the formation of a high temperature phase, a third polymorph of 1:2 GA–SM co-crystal. This new polymorph, designated as polymorph III, is thus formed from polymorph I and only exists at high temperature. The melting peak observed in the DSC of polymorph I (red trace in Figure 13a) therefore corresponds to the melting of polymorph III. Establishing enantiotropy/monotropy among the polymorphs has several cautions in the literature^{10f,15,16} and will be unambiguous only when the DSC measurements are performed in uniform and rigorous conditions for all the polymorphs considered. Herein, since different heating rates were applied for different polymorphs and polymorph II could not be reproduced for more experimentation, we refrain from establishing enantiotropic/monotropic relationship as the interpretation with limited data is prone to erratic conclusions. Based on the heat of fusion values obtained (Table 4), the stability order for the polymorphs at 0 K can be inferred as II (most stable) > I > III (least stable).

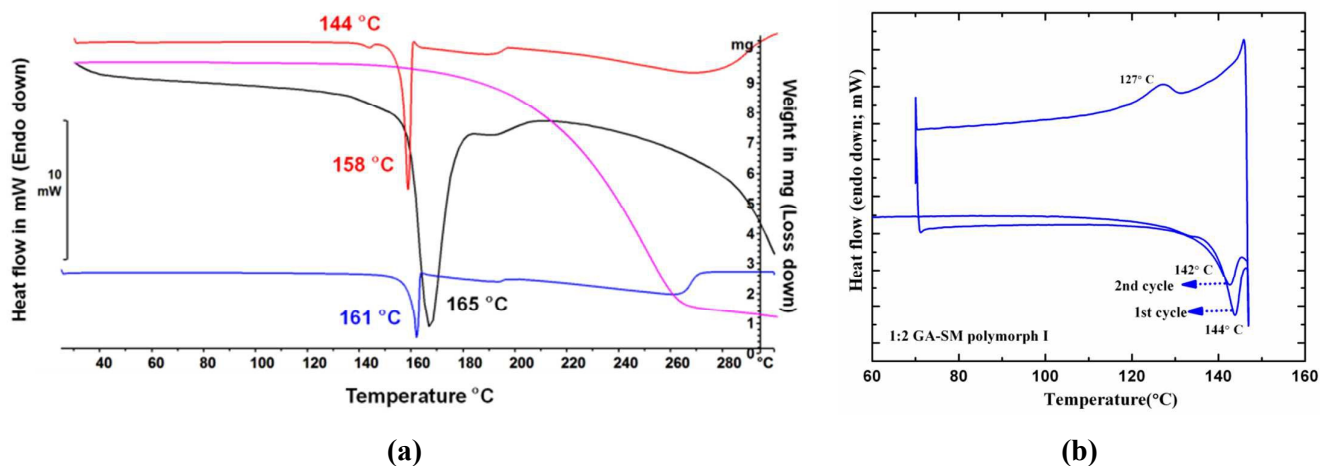


Figure 13 (a) DSC plots of 1:2 GA–SM co-crystal polymorphs I (red: @ 5 °C/min; black: @ 100 °C/min) and II (blue: @ 5 °C/min). The small endotherm at 144 °C in polymorph I (red) indicates polymorphic transformation before melting (158 °C) since there is no weight loss in TGA (magenta) pertaining to the endothermic transition. DSC of polymorph I at high heating

rate (black) resulted in its melting at 165 °C. Polymorph II (blue) shows clean melting at 161 °C. **(b)** Heat-cool-reheat DSC plot of 1:2 GA–SM co-crystal polymorph I shows endo-exo-endo peaks pertaining to reversible polymorphic transformation to a high temperature phase which actually melts at 158 °C (red trace).

Table 4 Thermal data of 1:2 GA–SM co-crystal polymorphs.

Polymorph	Heating rate (°C/min)	T_m (°C)	ΔH_{fus} (kJ/mol)
I	100	165	47.4
II	5	161	55.5
III	5	158	44.4

Conclusions

Crystal form diversity in terms of polymorphs and pseudopolymorphs of the GA–SM co-crystal along with its variable stoichiometry co-crystals has been extensively studied. A rare phenomenon of concomitant solvation for GA–SM 1:2 co-crystal, apart from its concomitant polymorphism was encountered. Further, the hydration/solvation tendency of 1:1 co-crystal makes it elusive to be obtained in pure state from routine crystallization experiments. Starting with the supramolecular building blocks for GA–SM combination, the structural reasons for concomitant solvation and polymorphism of 1:2 co-crystal and hydration/solvation of 1:1 co-crystal were uncovered. Furthermore, several pseudopolymorphs of the co-crystal could be designed and the logistics ensured successful preparation of phase-pure 1:2 and 1:1 co-crystals. Thus, this study deals nemesiss issues of co-crystallization, a feature of extreme importance to pharmaceutical industry, with implications in comprehending the goal of making desired materials.

Experimental Section

Materials: Commercially available compounds (Sigma-Aldrich, Bengaluru, India) were used without further purification. Solvents were of analytical or chromatographic grade and purchased from local suppliers. Water purified from a Siemens Ultra Clear water purification system was used for experiments.

Methods

Grinding: Compounds in molar ratios combined on the 100 mg scale were subjected to both neat and liquid-assisted grinding for 15 min using a mortar-pestle. Nitrogen atmosphere for grinding experiments was created by discharging ultra high pure nitrogen through a big funnel connected to the line inside a fume hood.

Evaporative Crystallization: Ground mixtures of GA–SM combination were kept for crystallization at ambient conditions in different solvents viz. methanol, ethanol, acetone (Act), THF, 1,4-dioxane (14D), acetonitrile, EtOAc, DMF, DMSO etc.

1:1:1 GA–SM–H₂O, 2:2:1 GA–SM–H₂O & 2:4:1 GA–SM–H₂O: Ground mixture of GA (17 mg, 0.1 mmol) and SM (10 mg, 0.1 mmol) was dissolved in 5 mL methanol and left for slow evaporation. All these hydrates harvested as colorless plates along with colorless needles of 1:2 GA–SM co-crystal polymorph I after a few days upon solvent evaporation.

1:1:1 GA–SM–14D: Ground mixture of GA (17 mg, 0.1 mmol) and SM (10 mg, 0.1 mmol) was dissolved in 5 mL 1,4-dioxane. Colorless block crystals of the solvate were obtained concomitantly along with colorless needles of 1:2 GA–SM co-crystal polymorph I after a few days upon solvent evaporation.

2:2:1 GA–SM–Act: Ground mixture of GA (17 mg, 0.1 mmol) and SM (10 mg, 0.1 mmol) was dissolved in 5 mL acetone. Colorless needle crystals of the solvate were obtained after a few days upon solvent evaporation. Since 1:2 GA–SM co-crystal polymorph I also crystallizes as needles and therefore poses difficulty in the identification of the solvate, all the harvested crystals were carefully screened and crystal data was collected. On the other hand, our attempts to reproduce the solvate were unsuccessful and later crystallization experiments resulted in only 1:2 GA–SM co-crystal polymorph I.

2:2:1 GA–SM–THF: Ground mixture of GA (17 mg, 0.1 mmol) and SM (10 mg, 0.1 mmol) was dissolved in 5 mL tetrahydrofuran to harvest colorless needles of the solvate. Observations similar to that of acetone solvate were noted in this case with regard to crystal morphology and irreproducibility.

3:3:1 GA–SM–EtOAc: Ground mixture of GA (17 mg, 0.1 mmol) and SM (10 mg, 0.1 mmol) was dissolved in 5 mL ethylacetate. Colorless block crystals of the solvate were obtained concomitantly along with colorless needles of 1:2 GA–SM co-crystal polymorph I after a few days upon solvent evaporation.

Vapor diffusion experiments: 100 mg of each of the solvate powder materials was spread in a Petri plate and exposed to vapors of other solvents (of 5 mL contained in a beaker) inside standard glass desiccators (1:1:1 GA–SM hydrate independently with 1,4-dioxane and ethyl acetate; 1:1:1 GA–SM–14D with water and ethyl acetate; 3:3:1 GA–SM–EtOAc with water and 1,4-dioxane). The materials were left undisturbed until complete evaporation of the solvent and later were analyzed by PXRD for any transformation to other solvates.

Single crystal X-ray diffraction: X-ray reflections on suitable single crystals were collected on an Oxford Xcalibur (Mova) diffractometer equipped with an EOS CCD detector and a

microfocus sealed tube using Mo K α radiation ($\lambda = 0.71073 \text{ \AA}$). Low temperature data collection was performed using an Oxford cobra open stream non-liquid nitrogen cooling device. Data collection and reduction was performed using CrysAlisPro (version 1.171.36.32)¹⁷ and OLEX2 (version 1.2)¹⁸ was used to solve and refine the crystal structures. All non-hydrogen atoms were refined anisotropically. Hydrogen atoms on O and N were located from difference electron density maps and all C–H atoms were fixed geometrically using HFIX command. The WinGX package¹⁹ was used for final refinement and production of CIFs and crystallographic parameters table. 3:3:1 GA–SM–EtOAc solvate showed a positional disorder with respect to carbonyl oxygen of the solvent molecule which was resolved by refining it with occupancy of 90:10. Both the oxygen atoms of solvent molecules were kept isotropic during the refinements.

Powder X-ray Diffraction: PXRD were recorded on PANalytical X'Pert diffractometer using Cu-K α X-radiation ($\lambda = 1.54056 \text{ \AA}$) at 40 kV and 30 mA. X'Pert HighScore Plus (version 1.0d)²⁰ was used to collect and plot the diffraction patterns. Diffraction patterns were collected over 2θ range of 5–40° using a step size of 0.06° 2θ and time per step of 1 sec.

NMR spectroscopy: Solution state ¹H NMR spectrum was recorded on a Bruker Avance spectrometer at 400 MHz using DMSO-d₆ as solvent.

1:1 GA–SM: δ (ppm): 2.55 (4H, s), 6.90 (2H, s), 8.77 (1H, s), 9.13 (2H, s), 11.03 (1H, s), 12.17 (1H, s).

Thermal analysis: DSC was performed on a Mettler Toledo DSC 822e module and TGA on a Mettler Toledo TGA/SDTA 851e module. High heating rate (100 °C/min) DSC experiment was performed on Mettler Toledo DSC 1 module. The typical sample size is 1–3 mg for DSC and 3–5 mg for TGA. The temperature range used in both DSC and TGA is 25–350 °C, and the samples were heated @ 5 °C/min. Samples were placed in crimped but vented aluminum pans for DSC and open alumina pans for TGA and were purged by a stream of dry nitrogen flowing at 50 mL/min.

Packing Diagrams: X-Seed was used to prepare packing diagrams.²¹

Lattice energy calculations: The lattice energy of a molecular crystal is the energy difference between the total energy of the unit cell and the isolated single molecule in the gas phase. It corresponds to the packing energy due to the interactions among the molecules in the crystal. For comparatively rigid molecules (i.e. those having almost similar geometry in gas phase and in crystal) the cohesive energy expression reduces to:

$$E(\text{lattice energy}) = \Delta E(\text{cond}) + \text{BSSE},$$

where, $\Delta E(\text{cond}) = E(\text{bulk})/Z - E(\text{mol, bulk})$, $\text{BSSE} = E(\text{mol, bulk}) - E(\text{mol, ghost})$

The terms have the following meanings:

$E(\text{bulk})$ = Total energy of the unit cell and must be referred to the value of Z (Z = the number of molecules in the unit cell).

$E(\text{mol, bulk})$ = Energy associated with a single molecule having the same geometry as in the bulk.

$E(\text{mol, ghost})$ = Calculated energy of a single molecule with augmented basis set by using ghost functions on the surrounding atoms.

These calculations were carried out on 1:2 GA–SM co-crystal polymorphs I & II using CRYSTAL09 at the DFT (B3LYP) level of theory using the 6-31G** basis set.²² The calculations were performed using the coordinates obtained from the experimental X-ray crystal structures of the polymorphs^{6f} determined at 130 K and 110 K respectively. The X–H bonds were neutron normalized prior to calculations.

† CCDC Nos. 1413790-1413796. These data are available at www.rsc.org.

Acknowledgements

RPK thanks the Institute for a Senior Research Fellowship and SC thanks the UGC for a Dr. D. S. Kothari Postdoctoral Fellowship. PBM thanks DST-IRHPA for project assistantship. TNG thanks the DST for a J. C. Bose Fellowship. We thank Prof. Ashwini Nangia for his help in recording high heating rate DSC experiment at Central Instruments Laboratory (CIL), University of Hyderabad. We thank the Institute for providing infrastructure and instrumentation facilities.

Notes and References

1 (a) N. Blagden and R. J. Davey, *Cryst. Growth Des.*, 2003, **3**, 873; (b) M. Habgood, M. A. Deij, J. Mazurek, S. L. Price and J. H. ter Horst, *Cryst. Growth Des.*, 2010, **10**, 903; (c) K. S. Eccles, R. E. Deasy, L. Fábíán, D. E. Braun, A. R. Maguire and S. E. Lawrence, *CrystEngComm*, 2011, **13**, 6923; (d) A. Mukherjee and G. R. Desiraju, *Chem. Commun.*, 2011, **47**, 4090; (e) A. Mukherjee, P. Grobelny, T. S. Thakur, and G. R. Desiraju, *Cryst. Growth Des.*, 2011, **11**, 2637; (f) S. Tothadi and G. R. Desiraju, *Phil. Trans. R. Soc. A*, 2012, **370**, 2900; (g) O. G. Uzoh, A. J. Cruz-Cabeza and S. L. Price, *Cryst. Growth Des.*, 2012, **12**, 4230; (h) C. B. Aakeröy, P. D. Chopade, C. Ganser, A. Rajbanshi and J. Desper, *CrystEngComm*, 2012, **14**, 5845; (i) R. M. Bhardwaj, L. S. Price, S. L. Price, S. M. Reutzeldens, G. J. Miller, I. D. H. Oswald, B. F. Johnston and A. J. Florence, *Cryst. Growth*

Des., 2013, **13**, 1602; (j) S. Z. Ismail, C. L. Anderton, R. C. B. Copley, L. S. Price and S. L. Price, *Cryst. Growth Des.*, 2013, **13**, 2396; (k) R. Dubey, M. S. Pavan, T. N. G. Row and G. R. Desiraju, *IUCrJ*, 2014, **1**, 8; (k) S. SeethaLekshmi, S. Varughese, L. Giri and V. R. Pedireddi, *Cryst. Growth Des.*, 2014, **14**, 4143; (l) A. Lemmerer and M. A. Fernandes, *New J. Chem.*, 2012, **36**, 2242.

2(a)http://www.ema.europa.eu/docs/en_GB/document_library/Scientific_guideline/2014/07/WC500170467.pdf (accessed on 06 October, 2015);

(b)<http://www.fda.gov/downloads/Drugs/Guidances/UCM281764.pdf> (accessed on 06 October, 2015); (c) Ö. Almarsson, M. L. Peterson and M. J. Zaworotko, *Pharm. Pat. Anal.*, 2012, **3**, 313; (d) T. Friščić and W. Jones, *J. Pharm. Pharmacol.*, 2010, **62**, 1547; (e) N. Schultheiss and A. Newman, *Cryst. Growth Des.*, 2009, **9**, 2950; (f) N. Blagden, M. de Matas, P. T. Gavan, and P. York, *Adv. Drug Deliv. Rev.*, 2007, **59**, 617.

3 (a) K. H.-Y. Hsi, K. Chadwick, A. Fried, M. Kenny and A. S. Myerson, *CrystEngComm*, 2012, **14**, 2386; (b) T. Lee, H. R. Chen, H. Y. Lin and H. L. Lee, *Cryst. Growth Des.*, 2012, **12**, 5897; (c) K. Kodama, E. Sekine and T. Hirose, *Chem. Eur. J.*, 2011, **17**, 11527; (d) J. Urbanus, C. P. M. Roelands, D. Verdoes, P. J. Jansens, and J. H. ter Horst, *Cryst. Growth Des.*, 2010, **10**, 1171.

4 (a) W. Zhu, R. Zheng, X. Fu, H. Fu, Q. Shi, Y. Zhen, H. Dong and W. Hu, *Angew. Chem. Int. Ed.*, 2015, **54**, 6785; (b) G. Griffini, L. Brambilla, M. Levi, C. Castiglioni, M. D. Zoppo and S. Turri, *RSC Adv.*, 2014, **4**, 9893; (c) R. Kaur, S. S. R. R. Perumal, A. J. Bhattacharya, S. Yashonath and T. N. G. Row, *Cryst. Growth Des.*, 2014, **14**, 423; (d) S. Horiuchi, R. Kumai and Y. Tokura, *J. Am. Chem. Soc.*, 2013, **135**, 4492; (e) S. K. McNeil, S. P. Kelley, C. Beg, H. Cook, R. D. Rogers and D. E. Nikles, *ACS Appl. Mater. Interfaces*, 2013, **5**, 7647; (f) M. Dong, Y.-W. Wang, A.-J. Zhang and Y. Peng, *Chem. Asian J.*, 2013, **8**, 1321; (g) T. E. Keyes, R. J. Forster, A. M. Bond and W. Miao, *J. Am. Chem. Soc.*, 2001, **123**, 2877; (h) D.-K. Bučar, S. Filip, M. Arhangelskis, G. O. Lloyd and W. Jones, *CrystEngComm*, 2013, **15**, 6289.

5 (a) B. Badhani, N. Sharma and R. Kakkar, *RSC Adv.*, 2015, **5**, 27540; (b) A. P. Subramanian, A. A. John, M. V. Vellayappan, A. Balaji, S. K. Jaganathan, E. Supriyanto and M. Yusof, *RSC Adv.*, 2015, **5**, 35608; (c) G.-C. Yena, P.-D. Duh and H.-L. Tsai, *Food Chem.*, 2002, **79**, 307.

6 (a) E. Lindpaintner, *Mikrochim. Acta*, 1939, **27**, 21; (b) D. E. Braun, R. M. Bhardwaj, A. J. Florence, D. A. Tocher and S. L. Price, *Cryst. Growth Des.*, 2013, **13**, 19; (c) H. D. Clarke, K. K. Arora, Ł. Wojtas and M. J. Zaworotko, *Cryst. Growth Des.*, 2011, **11**, 964; (d) R. Kaur

and T. N. G. Row, *Cryst. Growth Des.*, 2012, **12**, 2744; (e) S. P. Thomas, R. Kaur, J. Kaur, R. Sankolli, S. K. Nayak and T. N. G. Row, *J. Mol. Struct.*, 2013, **1032**, 88; (f) R. Kaur, R. Gautam, S. Cherukuvada and T. N. G. Row, *IUCrJ*, 2015, **2**, 341.

7 (a) S. Aitipamula, P. S. Chow and R. B. H. Tan, *CrystEngComm*, 2014, **16**, 3451; (b) S. Aitipamula, P. S. Chow and R. B. H. Tan, *Cryst. Growth Des.*, 2010, **10**, 2229; (c) N. J. Babu, L. S. Reddy, S. Aitipamula and A. Nangia, *Chem. Asian J.*, 2008, **3**, 1122; (d) B. R. Sreekanth, P. Vishweshwar and K. Vyas, *Chem. Commun.*, 2007, 2375; (e) H. D. Clarke, K. K. Arora, H. Bass, P. Kavuru, T. T. Ong, T. Pujari, L. Wojtas and M. J. Zaworotko, *Cryst. Growth Des.*, 2010, **10**, 2152; (f) G. R. Desiraju, J. J. Vittal and A. Ramanan, *Crystal Engineering: A Textbook*, World Scientific, 2011; (g) H. G. Brittain, *J. Pharm. Sci.*, 2012, **101**, 464; (h) P. Vishweshwar, J. A. McMahon, J. A. Bis and M. J. Zaworotko, *J. Pharm. Sci.*, 2006, **95**, 499; (i) S. L. Childs, P. A. Wood, N. Rodríguez-Hornedo, L. S. Reddy and K. I. Hardcastle, *Cryst. Growth Des.*, 2009, **9**, 1869; (j) S. P. Kelley, A. Narita, J. D. Holbrey, K. D. Green, W. M. Reichert and R. D. Rogers, *Cryst. Growth Des.*, 2013, **13**, 965; (k) Y. Qiu, Y. Chen and G. G. Z. Zhang, Eds., *Developing Solid Oral Dosage Forms. Pharmaceutical Theory and Practice*, Academic Press, New York, 2009; (l) G. M. Day, A. V. Trask, W. D. S. Motherwell and W. Jones, *Chem. Commun.*, 2006, 54; (m) P. Vishweshwar, J. A. McMahon, M. Oliveira, M. L. Peterson and M. J. Zaworotko, *J. Am. Chem. Soc.*, 2005, **127**, 16802.

8 (a) R. Thakuria, S. Cherukuvada and A. Nangia, *Cryst. Growth Des.*, 2012, **12**, 3944; (b) C. P. Brock and L. L. Duncan, *Chem. Mater.*, 1994, **6**, 1307; (c) A. Gavezzotti and G. Fillippini, *J. Phys. Chem.*, 1994, **98**, 4831; (d) K. M. Steed and J. W. Steed, *Chem. Rev.*, 2015, **115**, 2895.

9 S. Bhattacharya and B. K. Saha, *Cryst. Growth Des.*, 2013, **13**, 606.

10 (a) H. G. Brittain, Ed., *Polymorphism in Pharmaceutical Solids*, Informa Healthcare USA Inc., New York, 2009. (b) K. Kachrimanis, K. Fucke, M. Noisternig, B. Siebenhaar and U. J. Griesser, *Pharm. Res.*, 2008, **25**, 1440; (c) R. Hilfiker, Ed., *Polymorphism in the Pharmaceutical Industry*, Wiley-VCH, Weinheim, Germany, 2006. (d) A. Nangia, *Cryst. Growth Des.*, 2006, **6**, 2; (e) C. R. Gardner, C. T. Walsh and Ö. Almarsson, *Nat. Rev. Drug Disc.*, 2004, **3**, 926; (f) J. Bernstein, *Polymorphism in Molecular Crystals*, Clarendon, Oxford, U. K., 2002. (g) S. R. Chemburkar, J. Bauer, K. Deming, H. Spiwek, K. Patel, J. Morris, R. Henry, S. Spanton, W. Dziki, W. Porter, J. Quick, P. Bauer, J. Donaubaue, B. A. Narayanan, M. Soldani, D. Riley and K. McFarland, *Org. Process Res. Dev.*, 2000, **4**, 413. (h) C. Witschi and E. Doelker, *Eur. J. Pharm. Biopharm.*, 1997, **43**, 215.

11 (a) A. Delori, T. Friščić and W. Jones, *CrystEngComm*, 2012, **14**, 2350; (b) D. Braga, L. Maini and F. Grepioni, *Chem. Soc. Rev.*, 2013, **42**, 7638; (c) A. V. Trask and W. Jones, *Top. Curr. Chem.*, 2005, **254**, 41; (d) N. Shan, F. Toda and W. Jones, *Chem. Commun.*, 2002, 2372; (e) M. C. Etter and G. M. Frankenbach, *Chem. Mat.*, 1989, **1**, 10.

12 (a) W. F. Ostwald, *Z. Phys. Chem.*, **1897**, 22, 289; (b) J. Nývlt, *Cryst. Res. Technol.*, 1995, **30**, 443; (c) T. Threlfall, *Org. Pro. Res. Dev.*, 2003, **7**, 1017.

13 B. P. van Eijck and J. Kroon, *Acta Crystallogr.*, 2000, **B56**, 535.

14 J. M. Miller, N. Rodríguez-Hornedo, A. C. Blackburn, D. Macikenas and B. M. Collman, In *Solvent Systems and Their Selection in Pharmaceutics and Biopharmaceutics*, Springer, AAPS Press, New York, 2007, 53.

15 (a) T. L. Threlfall, *Org. Pro. Res. Dev.*, 2009, **13**, 1224; (b) T. Hino, J. L. Ford and M. W. Powell, *Thermochim. Acta*, 2001, **374**, 85; (c) D. Giron, *Thermochim. Acta*, 1995, **248**, 1; (d) L. Yu, *J. Pharm. Sci.*, 1995, **84**, 966; (e) J. B. Nanubolu, B. Sridhar, K. Ravikumar, K. D. Sawant, T. A. Naik, L. N. Patkar, S. Cherukuvada and B. Sreedhar, *CrystEngComm*, 2013, **15**, 4448; (f) N. Zencirci, T. Gelbrich, D. C. Apperley, R. K. Harris, V. Kahlenberg and U. J. Griesser, *Cryst. Growth Des.*, 2010, **10**, 302. (g) J. Haleblian and W. McCrone, *J. Pharm. Sci.*, 1969, **58**, 911; (h) A. Burger and R. Ramberger, *Microchim. Acta*, 1979, **72**, 259.

16. Several cautions in establishing enantiotropy/monotropy between the polymorphs observed in the literature^{10f,15} are: (i) Routine DSC measurements, which are generally done from room temperature and using 10 K/min heating rate, suffer from bias since a phase transition can be at low temperature or may be unobserved because of slow transition rate; (ii) The slope/curvature of a typical phase diagram is a schematic and can be skewed such that the 'heat of fusion rule'^{15h} for establishing thermodynamic stability is not universal and exceptions are possible; (iii) Melting temperatures of different polymorphs obtained from different heating rates cannot be compared and considered for establishing polymorphs as low/high melting ones. This is because different rates of heating can give different melting temperatures for the same polymorph such that interpretation from 'heat of fusion rule' becomes ambiguous. However, heat of fusion values integrated for different heating rate DSC measurements remain almost same and therefore can be used to establish stability order among polymorphs.

17 CrysAlisPro, ver. 1.171.36.32, (2011). Agilent Technologies UK Ltd: Yarnton, England.

18 O. V. Dolomanov, A. J. Blake, N. R. Champness and Schröder, *M. J. Appl. Cryst.*, 2003, **36**, 1283.

19 L. J. Farrugia, *J. Appl. Cryst.*, 1999, **32**, 837.

20 *X'Pert HighScore Plus*, The complete powder analysis tool, PANalytical B. V. 2003.

21 L. J. Barbour, *X-Seed, Graphical Interface to SHELX-97 and POV-Ray, Program for Better Quality of Crystallographic Figures*, University of Missouri-Columbia, Columbus, MO, 1999.

22 V. R. Saunders, R. Dovesi, C. Roetti, R. Orlando, C. M. Z. Wilson, N. M. Harrison, K. Doll, B. Civalleri, I. Bush, P. D'Arco and M. Llunell, *User's Manual*; University of Torino: Torino, 2009.

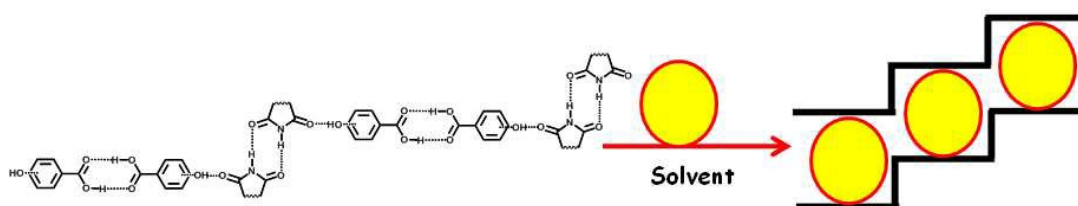
Gallic acid–Succinimide Co-crystal landscape: Polymorphism,
Pseudopolymorphism, Variable Stoichiometry Co-crystals and Concomitant
Growth of Non-solvated and Solvated Co-crystals

Ramanpreet Kaur, Suryanarayan Cherukuvada, Praveen B. Managutti and Tayur N. Guru

Row*

Solid State and Structural Chemistry Unit, Indian Institute of Science,
Bengaluru 560012, India

Table of Contents Graphic and Synopsis



A design aspect for selective formation of diverse solid forms such as solvates, hydrates and anhydrous forms has been successfully investigated in Gallic acid–Succinimide co-crystal landscape. Structural reasons for the rare phenomenon of concomitant growth of solvated and non-solvated co-crystals and the methods undertaken to resolve them have been explored systematically.